International Journal of Mass Spectrometry 304 (2011) 148–153

Contents lists available at ScienceDirect

International Journal of Mass Spectrometry

journal homepage: www.elsevier.com/locate/ijms

Non-covalent complexes between single-stranded oligodeoxynucleotides and poly(ethylene imine)

Danijela Smiljanic, Chrys Wesdemiotis*

Department of Chemistry, The University of Akron, Akron, OH 44325, USA

ARTICLE INFO

Article history:
Received 4 May 2010
Received in revised form 23 June 2010
Accepted 25 June 2010
Available online 3 July 2010

Keywords:
Polymer
Oligonucleotide
Non-covalent complexes
Solution vs. gas-phase stability
Gene delivery

ABSTRACT

Non-covalent complexes between low molecular weight poly(ethylene imine) (PEI 400 and 800) and single-stranded oligodeoxynucleotides (ODNs) were prepared in aqueous solution by combining polymer and ODN in molar ratios ranging from 1:10 to 10:1. Five ODNs were investigated, including d(TTTTT), d(CCCCC), d(AAAAA), d(GGGGG) and d(GCGAT). The compositions, solution stabilities and gas-phase stabilities of the complexes (termed polyplexes) were examined by electrospray ionization mass spectrometry (ESI-MS) and tandem mass spectrometry (MS^2). Independent of the mixing ratio of the reactants, the polyplex with 1:1 polymer-to-nucleotide stoichiometry, PN, is the dominant product, while the polyplexes PN_2 and P_2N are observed as byproducts with all ODNs. The relative polyplex ion abundances in the ESI mass spectra reveal the following order of solution stabilities for the major product PN: PEI-d(TTTTT) > PEI-d(GGGGG) ≈ PEI-d(GCGAT) ≈ PEI-d(CCCCC) > PEI-d(AAAAA). The gas-phase stabilities, assessed by MS^2 and collisionally activated dissociation, follow the same order, providing evidence that the polyplex structures in aqueous solution and the more hydrophobic environment of the gas-phase are very similar. PEI 800 leads to more stable polyplexes than PEI 400. PEI–ODN polyplexes have been used in gene delivery. The particularly high binding affinity of d(TTTTT) vs. the other ODNs suggests that sequence-specific delivery systems could be developed by appropriate design of the size and composition of the polymeric delivery vehicle.

1. Introduction

Gene therapy involves the delivery of appropriate genetic material to target cells, where it may replace defect genetic material, inhibit the production of a deleterious protein or cause the production of a therapeutic protein [1]. Cationic polymers, such as poly(ethylene imine) (PEI), are increasingly explored as delivery vehicles (vectors) of genes or oligonucleotides to cells, as they are less cytotoxic, less costly, and more easily prepared than traditionally used viral vectors [1–6]. Cationic polymers are positively charged at physiological pH and, thus, can develop attractive electrostatic interactions with nucleic acids and oligonucleotides, which generally carry negative charges [1]. The resulting complexes have been termed polyplexes and usually have a net positive charge, which helps them to penetrate the negatively charged cell membrane and escape degradation until they reach their ultimate destination, the cell nucleus [1,2,5].

Although a number of studies have been reported about the cytotoxicity, transfection efficiency and degradability of polyplexes [1,2,5], information about their compositions and binding interactions at the molecular level is scarce [4,7]. This issue is addressed here with the first characterization of PEI/oligodeoxynucleotide (ODN) polyplexes by electrospray ionization mass spectrometry (ESI-MS) [8], tandem mass spectrometry (MS^2) and traveling wave ion mobility mass spectrometry (TWIM-MS) [9]. The stoichiometry and charge state distributions of the complexes formed by PEI 400 and PEI 800 with a series of single-stranded pentadeoxynucleotides are examined, as are the corresponding complex stabilities in solution and the solvent-free environment.

2. Materials and methods

2.1. Materials

PEI 400 and PEI 800 were acquired from Sigma/Aldrich (Milwaukee, WI) and BASF (Ludwigshafen, Germany), respectively, and aqueous ammonium hydroxide (28–30%) from EMD Chemicals (Gibbstown, NJ). HPLC-grade water, ammonium acetate, the single-stranded pentadeoxynucleotides 5′-d(TTTTT)-3′, 5′-d(CCCCC)-3′, 5′-d(AAAAA)-3′, 5′-d(GGGGG)-3′ and 5′-d(GCGAT)-3′ were purchased from Fisher (Fair Lawn, NJ), as were all solvents.

* Corresponding author. Tel.: +1 330 972 7699; fax: +1 330 972 6085.
E-mail address: wesdemiotis@uakron.edu (C. Wesdemiotis).

1387-3806/$ – see front matter © 2010 Elsevier B.V. All rights reserved.
doi:10.1016/j.ijms.2010.06.035

All chemicals were used as received without further purification.

2.2. Sample preparation

A 10-mM ammonium acetate buffer was prepared in HPLC-grade water and its pH was adjusted to 7.2 by adding a few droplets of aqueous ammonium hydroxide. This buffer was used to prepare individual 0.5-mM solutions of the polymers and pentadeoxynucleotides. Polymer and nucleotide solutions were mixed in the ratios of 1:10, 1:5, 1:1, 5:1 or 10:1, and the resulting mixtures were introduced into the ESI source by direct infusion at a flow rate of 5 μL/min.

2.3. Mass spectrometry experiments

All experiments were performed with a Synapt HDMS quadrupole/time-of-flight (Q/ToF) tandem mass spectrometer (Waters, Beverly, MA) equipped with ESI and TWIM-MS capabilities [9,10]. The instrument contains a triwave device between the Q and ToF mass analyzers, consisting of three cells arranged in the order trap cell, ion mobility cell and transfer cell. ESI mass spectra were acquired in positive mode by setting the spray voltage at 3.5 kV, the source temperature at 110 °C, the sampling cone voltage at 35 V, the extraction cone voltage at 3.2 V, the desolvation gas flow rate at 400 L/h (N_2), the desolvation temperature at 160 °C, the quadrupole mass analyzer in RF-only mode, the trap cell collision energy at 4.0 eV and the transfer cell collision energy at 6.0 eV. Under these conditions, all ions leaving the ESI source pass the quadrupole and triwave regions and are orthogonally accelerated into the ToF mass analyzer for m/z analysis. For the acquisition of MS^2 spectra, a specific PEI–ODN complex (precursor ion) was mass-selected with Q using an isolation width of 4.5 and underwent collisionally activated dissociation (CAD) with Ar in the trap cell at an Ar gas flow of 1.5 mL/min. MS^2 (CAD) spectra were measured as a function of trap collision energy, which was varied within 6–45 eV to induce fragmentation. The product ions formed in this process were subsequently mass-analyzed by the ToF part.

Fragmentation efficiency curves were constructed from MS^2 spectra of $[M+2H]^{2+}$ ions by plotting the relative abundance of the selected PEI–ODN complex vs. the corresponding center-of-mass collision energy (E_{cm}) [11]. Relative abundance was calculated by dividing the complex intensity, $I(\text{complex}^{2+})$, by the sum $I(\text{complex}^{2+}) + 1/2\ [I(\text{PEI}^{+}) + I(\text{ODN}^{+})]$ [12,13]; E_{lab} was calculated from the applied laboratory-frame collision energy (E_{lab}) using the equation $E_{cm} = E_{lab} \times (m_{Ar}/(m_{Ar} + m_{precursor}))$, where m_{Ar} and $m_{precursor}$ designate the masses of Ar atoms and the precursor ion, respectively. The points were fitted into sigmoid curves, constructed using the Origin 8.1 graphing software [14], in order to deduce the corresponding E_{50} values, which are the collision energies at which 50% of the PEI–ODN precursor ions were depleted due to CAD [12,13,15]. The E_{50} value derived for each PEI–ODN complex is an average of three measurements.

The normalized intensities of the PEI–ODN complexes were used to determine the effect of solution phase composition on the stoichiometry of the resulting non-covalent complexes and the relative solution stabilities of the complexes [13,16–18]. Normalized intensities were obtained from peak heights by dividing the PEI–ODN complex intensity by that of uncomplexed ODN. The most abundant PEI–ODN oligomers (4 for PEI 400 and 12 for PEI 800) were used in this calculation. All detectable charge states of the PEI–ODN complexes and uncomplexed ODNs were considered. The uncomplexed ODNs dissociated partly during ESI analysis. The ODN fragment intensities were added to those of intact ODN for the calculation of normalized intensities.

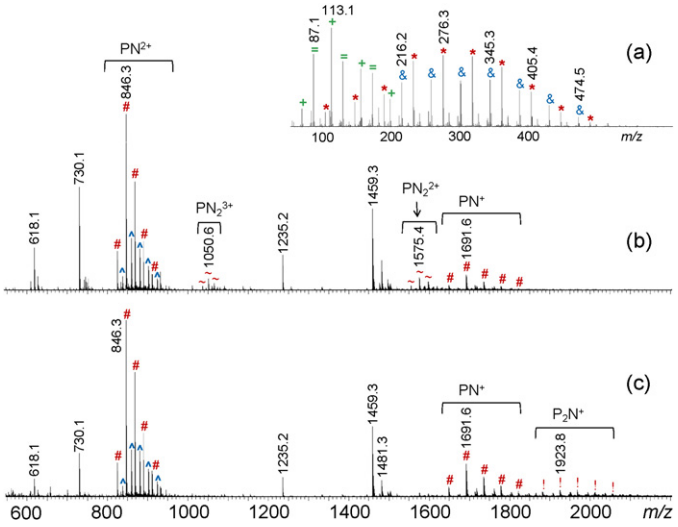

Fig. 1. ESI mass spectra of (a) PEI 400 and (b, c) the PEI–ODN polyplexes formed after mixing PEI 400 and 5′-d(TTTTT)-3′ in the molar ratios 1:1 (b) and 5:1 (c). The signs * and & designate $[M+H]^+$ ions of linear and cyclic PEI oligomers with the compositions $H_2N(CH_2CH_2NH)_nH$ and $(CH_2CH_2NH)_n$, respectively. The signs = and + designate PEI fragments with the compositions $H_2N(CH_2CH_2NH)_mCH_2CH_2NH^+{=}CHCH_3$ and $CH_3CH{=}N(CH_2CH_2NH)_mCH_2CH_2NH^+{=}CHCH_3$, respectively. The signs # and ∧ designate PEI-d(TTTTT) polyplexes containing linear (#) or cyclic (∧) PEI and having the PEI-to-ODN stoichiometry 1:1 (PN). The signs ∼ and ∧ designate polyplexes with the stoichiometries PN_2 (∼) or P_2N (!). The superscripted charges indicate degree of protonation. Monoisotopic m/z values are given on top of select peaks. The ions at m/z 1459.3 and 730.1 arise from singly and doubly protonated d(TTTTT), respectively, and the ions at m/z 1235.2 and 616.1 are the corresponding w_4^+/w_4^{2+} fragments.

Two-dimensional TWIM-MS plots were acquired on all ions exiting the ESI source (Q in RF-only mode), using a traveling wave velocity of 675 m/s and a traveling wave height of 17.2 V. The IM gas (N_2) flow was set at 22.7 mL/min and the trap and transfer cell potentials were kept at 6.0 and 4.0 V, respectively, during the IM measurement.

3. Results and discussion

3.1. Polyplexes with PEI 400

The poly(ethylene imine)s used for polyplex formation were supplied as mixtures of linear and branched oligomers; both have a 43-Da repeat unit, amine end groups and the nominal composition $H_2N(CH_2CH_2NH)_nH$. The $[M+H]^+$ ions of such oligomers give rise to the main distribution in the ESI mass spectrum of PEI 400, which appears m/z $43n + 18$ (labeled by * in Fig. 1a). A second distribution results from oligomers that are missing NH_3; these are observed at m/z $43n + 1$ (& in Fig. 1a) and agree well with cyclized structures, which are typical byproducts in PEI syntheses. Two more distributions are detected, mainly in the low-mass range; these correspond to PEI fragments formed during ESI (+ and = in Fig. 1a) [19]. The average molecular weight (M_n) calculated from the ESI mass spectrum for the main polymer distribution, i.e., for $H_2N(CH_2CH_2NH)_nH$, is 295; hence, the average PEI 400 oligomer contains 6–7 repeat units and 7–8 N atoms (potential protonation and hydrogen bonding sites).

PEI 400 was mixed with the pentadeoxynucleotides 5′-d(TTTTT)-3′, 5′-d(CCCCC)-3′, 5′-d(AAAAA)-3′, 5′-d(GGGGG)-3′ and 5′-d(GCGAT)-3′ in the molar ratios 10:1, 5:1, 1:1, 1:5 and 1:10. After the mixtures were allowed to equilibrate for 10 min, ESI mass spectra were acquired to identify the polyplexes formed. With all ODNs and molar ratios examined, the PEI–ODN polyplex with 1:1 stoichiometry is the dominant product, as attested in Fig. 1b and c for the PEI/d(TTTTT) complex formed from polymer-

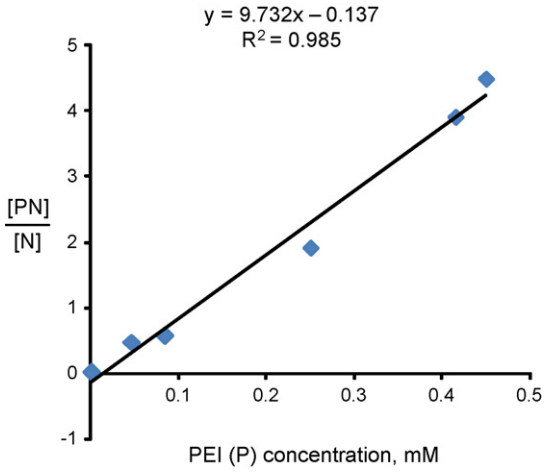

Fig. 2. Relative intensity of the PEI-d(TTTTT) polyplexes with polymer-to-ODN stoichiometry of 1:1 (PN) vs. the total PEI 400 concentration in the PEI/ODN solution.

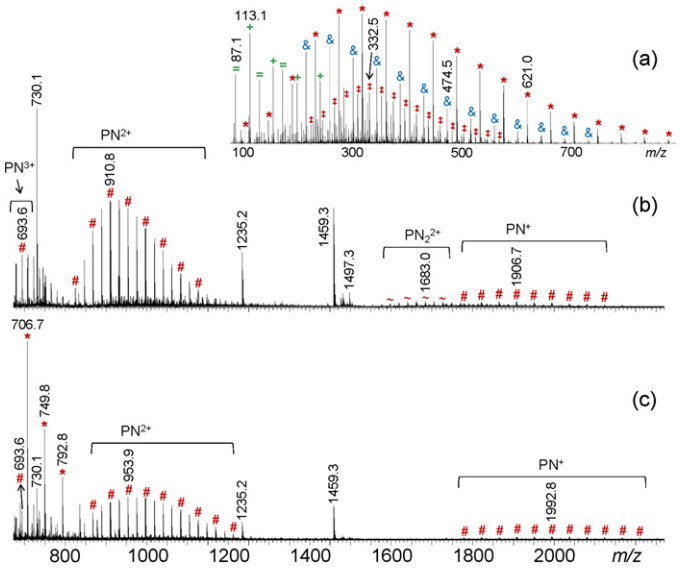

Fig. 3. ESI mass spectra of (a) PEI 800 and (b, c) the PEI–ODN polyplexes formed after mixing PEI 800 and 5′-d(TTTTT)-3′ in the molar ratios 1:1 (b) and 5:1 (c). The signs * and ‡ designate $[M+H]^+$ and $[M+2H]^{2+}$ ions, respectively, of linear PEI oligomers with the composition $H_2N(CH_2CH_2NH)_nH$; the sign & designates $[M+H]^+$ ions of cyclic PEI oligomers with the composition $(CH_2CH_2NH)_n$. The signs = and + designate PEI fragments with the compositions $H_2N(CH_2CH_2NH)_mCH_2CH_2NH^+{=}CHCH_3$ and $CH_3CH{=}N(CH_2CH_2NH)_mCH_2CH_2NH^+{=}CHCH_3$, respectively. The sign # designates PEI-d(TTTTT) polyplexes with the linear PEI oligomers and the PEI-to-ODN stoichiometry 1:1 (PN). The sign ~ designates polyplexes with the stoichiometry PN_2. The superscripted charges indicate degree of protonation. Monoisotopic m/z values are given on top of select peaks. The ions at m/z 1459.3 and 730.1 arise from singly and doubly protonated d(TTTTT), respectively, and the ion at m/z 1235.2 is the corresponding w_4^+ fragment. At the higher polymer concentration (bottom), heavier PEI oligomers (*) dominate in the low-mass end of the spectrum.

to-ODN ratios of 1:1 and 5:1, respectively. The 1:1 stoichiometry is observed in charge state +2, as $[M+2H]^{2+}$, as well as in charge state +1, as $[M+H]^+$, with the latter increasing in relative abundance at higher polymer-to-ODN molar ratios (cf. Fig. 1). For brevity, the notations PN^{2+} and PN^+ will be used for the polyplexes, with P and N representing the polymer and oligodeoxynucleotide, respectively, and the superscript providing the corresponding charge state. At higher ODN concentrations, doubly and triply protonated complexes with the stoichiometry PN_2 appear as minor product (Fig. 1b). Inversely, a higher polymer concentration coproduces small amounts of P_2N^{2+}/P_2N^+ complexes (Fig. 1c).

Both the major PEI distribution with the nominal composition $H_2N(CH_2CH_2NH)_nH$ (* in Fig. 1a) as well as the minor, cyclized PEI distribution (& in Fig. 1a) form complexes (# and ∧, respectively, in Fig. 1b and c). No complexes are observed with the PEI fragment series (+ and = in Fig. 1a). The fraction of polyplexes that contain cyclic PEI (∧) is somewhat smaller than the fraction of cyclic structures in PEI (&), pointing out that cyclic oligomers yield less stable complexes with ODNs.

Table 1 summarizes the relative intensities of the polyplexes obtained from mixtures with polymer-to-oligonucleotide molar ratios of 1:1 and 5:1. Only polyplexes containing the major PEI distribution were considered in the calculation of these intensities. The yield of the major product, viz. the PN complex with 1:1 polymer-to-oligonucleotide stoichiometry, increases significantly with the molar PEI/ODN ratio of the reactants, as expected. At all mixing ratios, the most abundant PN complex is observed for d(TTTTT), with the relative intensities of the other complexes following the order PEI-d(TTTTT) > PEI-d(GGGGG) ≈ PEI-d(CCCCC) ≈ PEI-d(GCGAT) > PEI-d(AAAAA). The relative intensities of the polyplexes correlate linearly with the PEI concentration; this is shown in Fig. 2 for the complex of d(TTTTT). Such relationship reveals that the ESI mass spectra provide snapshots of the PN/N solution concentrations and that the relative intensities of the PEI–ODN complexes reasonably approximate the corresponding relative solution stabilities (cf. footnote 'a' in Table 1). Based on this fact, the relative PN intensities in Table 1 indicate that d(TTTTT) produces the most stable and d(AAAAA) the least stable 1:1 polyplex with PEI, while the other pentadeoxynucleotides yield polyplexes of intermediate stability.

The most stable PN_2 complex is also formed with d(TTTTT), but the most stable P_2N complex is formed with d(GGGGG), cf. Table 1. Such a change in the order of polyplex stabilities could result from a change in the secondary ODN structure when a further constituent is added to the non-covalent complex.

It is noteworthy that the molecular weight distribution of the polyplexes is narrower than that of PEI 400 (cf. Fig. 1), indicating that only a select range of PEI sizes can form stable complexes with pentadeoxynucleotides. The number of ethylene imine repeat units in the four most abundant PN^{2+} ions is 4–7 for PEI-d(TTTTT), 5–8 for PEI-d(GGGGG), PEI-d(CCCCC) and PEI-d(GCGAT) and 6–9 for PEI-d(AAAAA), while the four most abundant ions within the corresponding PN^+ series carry 4–7 repeat units in all cases. From these data, the N-atom/P-atom ratios of the polyplexes can be calculated, which is defined as the number the N atoms in the PEI component divided by the number of P atoms in the nucleic acid component. Considering that non-cyclic PEIs contain one more N atom than their number of repeat units and that the number of P atoms in the ODNs studied is five, the N-atom/P-atom ratios of the polyplexes (PN stoichiometry) fall within the range (5–9)/5 = 1.0–1.8. For the in vivo or in vitro delivery of nucleic acids and oligodeoxynucleotides, N-atom/P-atom ratios of 5–10 or larger are generally used, which maximize polyplex formation according to agarose gel electrophoresis analyses [2,3,5,20]. The excess PEI, as compared to the complex stoichiometry, shifts the complexation equilibrium toward the polyplex and adds more positive charge which is believed to facilitate transfection through the cell membrane [1].

3.2. Comparison of PEI 400 vs. PEI 800

The ESI mass spectrum of PEI 800 (Fig. 3a) shows very similar characteristics to those described for PEI 400 (vide supra). The major distribution, appearing at m/z $43n + 18$, originates again from $[M+H]^+$ ions of amine-terminated oligomers which, as mentioned above, contain mixtures of linear and branched chains (each branch converts one CH_2CH_2NH subunit to CH_2CH_2N and another one to $CH_2CH_2NH_2$, which does not alter the overall PEI

Table 1
PEI–ODN (PN) polyplexes formed between PEI 400 and single-stranded pentadeoxynucleotides.

PEI/ODN mixing ratio	1:1		5:1	
Complex stoichiometry ODN (N)	1:1 [PN]/[N][a]	1:2 $[PN_2]/[N]$[b]	1:1 [PN]/[N][a]	2:1 $[P_2N]/[N]$[c]
5′-d(TTTTT)-3′	1.90	0.35	3.89	0.27
5′-d(CCCCC)-3′	0.41	0.09	1.06	0.25
5′-d(AAAAA)-3′	0.08	0.06	0.26	0.06
5′-d(GGGGG)-3′	0.55	0.18	1.17	0.63
5′-d(GCGAT)-3′	0.42	0.18	0.83	0.19

[a] $([PN^{2+}]+[PN^{+}])/[N]_{free}$ ($[N]_{free}$ is the sum of the intensities of all uncomplexed ODN species, viz. N^{2+}, N^{+} and their 2+/1+ fragments); ±10%. The complexation reaction $P+N \leftrightarrows PN$ is associated with an equilibrium constant (binding affinity) $K_b = [PN]/([N][P])$, with [N] and [P] representing the molar concentrations of free ODN and PEI, respectively. Rewriting this equation as $[PN]/[N] = K_b[P]$ shows that the [PN]/[N] concentration ratio is proportional to both the binding affinity K_b (a measure of the complex stability in solution) as well as the concentration of free polymer, [P], which increases with the total concentration of polymer (cf. Fig. 2).
[b] $([PN_2^{2+}]+[PN_2^{3+}])/[N]_{free}$; ±20%.
[c] $([P_2N^{+}]+[P_2N^{2+}])/[N]_{free}$; ±20%.

composition). The proportion of cyclized oligomers, observed at m/z $43n+1$, is smaller with PEI 800 than PEI 400; on the other hand, the larger poly(ethylene imine) generates a sizable $[M+2H]^{2+}$ distribution (~40% of the $[M+H]^{+}$ distribution), which was near noise level in the ESI mass spectrum of PEI 400 (cf. Fig. 1a). The average molecular weight (M_n) calculated from the singly and doubly protonated oligomers for the main polymer distribution, viz. $H_2N(CH_2CH_2NH)_nH$, is ~530, indicating that the average PEI 800 oligomer carries ~12 repeat units and ~13 N atoms.

It should be noted at this point that the M_n values obtained from the mass spectra are lower than those reported by the supplier (400 or 800), which were measured by gel permeation chromatography (GPC). Aggregation due to hydrogen bonding could cause the overestimation in the GPC results [21,22].

The effect of increasing the molecular weight of the poly(ethylene imine) carrier was tested with d(TTTTT). Fig. 3b and c show the ESI mass spectra obtained if polymer and ODN are mixed in molar ratios of 1:1 and 5:1, respectively. As with PEI 400, the polyplex with 1:1 stoichiometry (PN) is the predominant (Fig. 3b) or solely detected (Fig. 3c) product. The PN complexes of PEI 800 form mainly doubly protonated PN^{2+} ions (as with PEI 400) along with some singly charged PN^{+} and triply charged PN^{3+}. The relative intensity of PN, calculated by adding the intensities of the PN complexes in all charge states and dividing the resulting sum by the intensity of free ODN and its fragments in all charge states, increases from 4.39 to 9.78 when the polymer-to-oligodeoxynucleotide ratio is increased from 1: 1 to 5:1; the corresponding values with PEI 400 were 1.90 and 3.89, respectively. The larger PN/N intensity ratios with PEI 800 indicate a higher stability for the polyplexes with PEI 800, most likely because the higher number of basic and hydrogen bonding sites in the larger polymer leads to stronger non-covalent interactions and higher binding affinities.

PN complexes with 4–25 ethylene imine repeat units are detected in the spectra of Fig. 3. This range is comparable with the range of poly(ethylene imine) n-mers observed in the ESI mass spectrum of PEI 800 (n = 2–27). Thus, essentially the entire linear/branched PEI distribution reacts to form polyplexes. The average molecular weight (M_n) of the PEI attached to d(TTTTT), calculated from the PN^{2+} distributions in Fig. 3, is 480 when polymer and pentanucleotide are combined in the ratio of 1:1 (Fig. 3b) and 570 when the combination ratio is 5:1 (Fig. 3c). An increased PEI concentration (i.e., 5:1) favors disproportionally complexation with the heavier oligomers because of their higher binding affinities to d(TTTTT).

Interestingly, the cyclic components of PEI 800 do not react with d(TTTTT) to any appreciably degree (Fig. 3), in contrast to the cyclic components of PEI 400 which reacted (Fig. 1), albeit with an overall lower yield than the corresponding linear oligomers (vide supra). The increased binding affinities of larger linear/branched oligomers (more of them are present in PEI 800) and the poorer binding affinities of cyclic structures (less are present in PEI 800) reconcile these differences.

3.3. Intrinsic stability of polyplexes

The single-stage ESI mass spectra discussed thus far reveal information about the relative solution stabilities of the polyplexes which, in turn, depend on the corresponding intrinsic (i.e., gas-phase) stabilities and on solvation effects. Intrinsic stabilities were independently assessed by tandem mass spectrometry (MS^2) experiments on PEI–ODN complexes with PEI 400. Specifically, PN^{2+} ions containing the 5-mer (i.e., $P = H_2N(CH_2CH_2NH)_5H$) were isolated and induced to decompose by collisionally activated dissociation (CAD). During this process, all PN^{2+} precursor ions examined undergo one major dissociation to yield their P^{+} and N^{+} constituents, as exemplified in Fig. 4 by the MS^2 (CAD) spectra of PEI-d(TTTTT) and PEI-d(GCGAT).

The MS^2 (CAD) spectra of PN^{2+} were acquired as a function of the center-of-mass collision energy (E_{cm}), in order to construct fragmentation efficiency curves. Fig. 5 shows three examples, referring to the polyplexes of d(TTTTT), d(GCGAT) and d(AAAAA). The collision energies causing 50% of the PN^{2+} precursor ions to dissociate, termed E_{50} energies, represent a measure of the corresponding intrinsic polyplex stabilities. The E_{50} values of the five PEI–ODN complexes studied (Table 2) indicate the intrinsic stability order PEI-d(TTTTT) > PEI-d(GGGGG) ≈ PEI-d(CCCCC) ≈ PEI-d(GCGAT) > PEI-d(AAAAA), which is identical with the solution

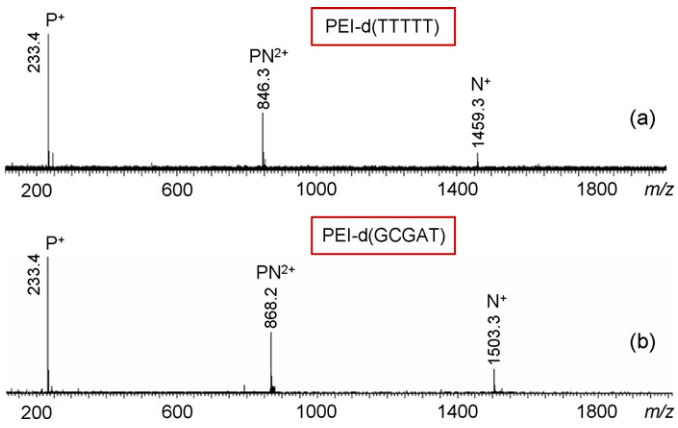

Fig. 4. MS^2 (CAD) mass spectra of PN^{2+} polyplex ions containing (a) d(TTTTT) and (b) d(GCGAT). The oligomers selected (m/z 846.7 and 868.2, respectively) contain 5 ethylene imine repeat units. The laboratory-frame collision energies were (a) 14 eV and (b) 13 eV.

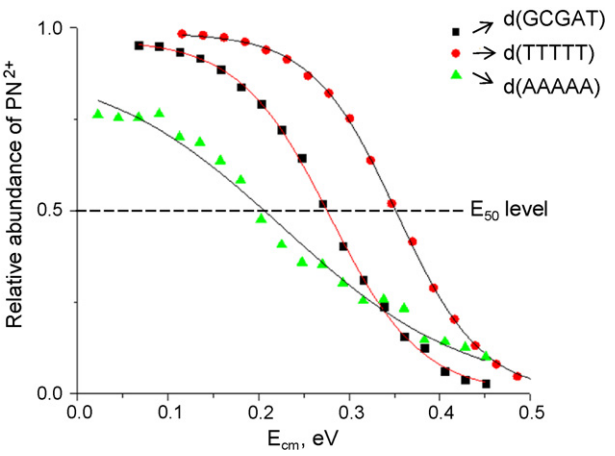

Fig. 5. Fragmentation efficiency curves (relative abundance of PN^{2+} precursor ion vs. center-of-mass collision energy) of polyplexes containing a PEI with 5 repeat units and d(TTTTT), d(AAAAA) or d(GCGAT).

Table 2
E_{50} values of PN^{2+} polyplexes between PEI 400 (P) and pentadeoxynucleotides (N).

ODN (N)	E_{50} (eV)[a]
5′-d(TTTTT)-3′	0.35
5′-d(CCCCC)-3′	0.29
5′-d(AAAAA)-3′	0.23
5′-d(GGGGG)-3′	0.29
5′-d(GCGAT)-3′	0.29

[a] ±0.04.

stability order of these polyplexes. Such agreement strongly suggests that the PEI–ODN complexes have similar structures in the gas-phase and in solution (at physiological conditions).

From the singly charged PN^+ distributions, only the polyplexes of d(TTTTT), d(AAAAA) and d(CCCCC) were sufficiently intense to produce MS^2 spectra with useable signal-to-noise ratios (Fig. 6). The complex of d(TTTTT) dissociates exclusively to P^+, whereas the complexes of d(AAAAA) and d(CCCCC) lead to mixtures of P^+ and N^+. Because of the absence of charge repulsion in PN^+, these ions require higher collision energies for dissociation into their constituents than PN^{2+} ions. Additionally, competitive and consecutive reactions become possible within the ODN component of PEI-d(CCCCC), cf. Fig. 6c. Due to these complications, energetics data were not derived from the singly protonated polyplexes.

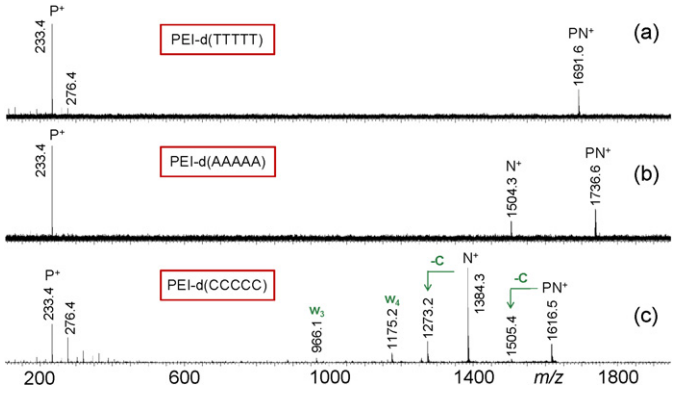

Fig. 6. MS^2 (CAD) mass spectra of PN^+ polyplex ions containing (a) d(TTTTT), (b) d(AAAAA) and (c) d(GGGGG). The oligomers selected (*m*/*z* 1691.6, 1736.6 and 1616.5, respectively) contain 5 ethylene imine repeat units. The laboratory-frame collision energies were (a, b) 38 eV and (c) 39 eV. The top and, especially, the bottom spectrum show a distribution of polymer ions, indicating admixtures in the selected PN^+ precursor ions (see ion mobility section).

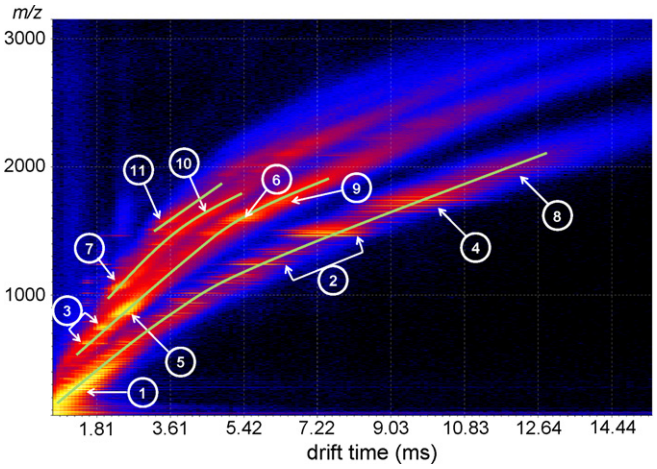

Fig. 7. Two-dimensional ESI-TWIM-MS plot (*m*/*z* vs. ion drift time) of the polyplexes formed after mixing PEI 400 and 5′-d(TTTTT)-3′ in the molar ratio 5:1. The regions marked by the encircled arrows correspond to: 1, protonated PEI (P^+); 2, singly protonated d(TTTTT), N^+, and $w_4{}^+$ fragment; 3, doubly protonated d(TTTTT), N^{2+}, and $w_4{}^{2+}$ fragment; 4, PN^+ polyplexes; 5, PN^{2+} polyplexes; 6, $PN_2{}^{2+}$ polyplexes; 7, $PN_2{}^{3+}$ polyplexes; 8, P_2N^+ polyplexes; 9, $P_2N_2{}^{2+}$ polyplexes; 10, $PN_3{}^{3+}$ polyplexes; 11, $P_4N_3{}^{4+}$ polyplexes. The four trend lines shown connect regions with identical charge states (+1 to +4 from right to left).

3.4. Ion mobility separation of the polyplexes

Ion mobility mass spectrometry (IM-MS) can separate ions according to their mass, charge and shape [23–34]. Charge- and shape-sensitive dispersion permits the separation of isomers and isobars and deconvolutes the isotope patterns of overlapping charge states, enhancing the resolving power and sensitivity of mass spectrometry. Traveling wave ion mobility mass spectrometry (TWIM-MS) [9,10], a recent variant of IM-MS, was employed to corroborate the presence of the polyplexes observed in the ESI mass spectra and identify any additional complex stoichiometries hidden under the dominating products. These experiments were performed with the PEI 400/d(TTTTT) system (polymer-to-ODN molar ratio 5:1), which yields the highest absolute intensities with the best signal-to-noise ratio.

Fig. 7 shows a two-dimensional TWIM-MS plot (*m*/*z* vs. drift time) for all ions exiting the ESI source. After IM separation through the traveling wave IM cell and *m*/*z* analysis by the orthogonal ToF analyzer, several families of ions could be identified, which have been marked 1–11. Fig. 8 shows the spectra of the regions which are not readily detected in the ESI mass spectrum because they have very small intensities and/or overlap with more abundant ions or other charge states.

Regions 1–3 contain the reactants; PEI is observed in region 1 (distributions as in Fig. 1a) and the ODN and its w_4 fragment in regions 2 (charge state +1) and 3 (charge state +2). All other areas contain non-covalent complexes, with the major PN polyplex appearing in region 4 (PN^+ distribution) and region 5 (PN^{2+} distribution). The minor products PN_2 and P_2N are detected in regions 6/7 and 8 in the form of $PN_2{}^{2+}/PN_2{}^{3+}$ and P_2N^+ distributions, respectively. All these ions were clearly discerned in the ESI mass spectrum of Fig. 1c. IM separation enables the detection of three further minor products in regions 9–11. The corresponding mass spectra confirm the compositions $P_2N_2{}^{2+}$ for region 9 (Fig. 8a), $PN_3{}^{3+}$ for region 10 (Fig. 8b) and $P_4N_3{}^{4+}$ for region 11 (Fig. 8c).

Ion drift times through the IM cell decrease with the number of charges due to the greater mobilities of the higher charge states in the traveling wave field. Different charge states follow distinct trend lines that are clearly separated from each other. Note that the PN^+ distribution of the major polyplex is superimposed with

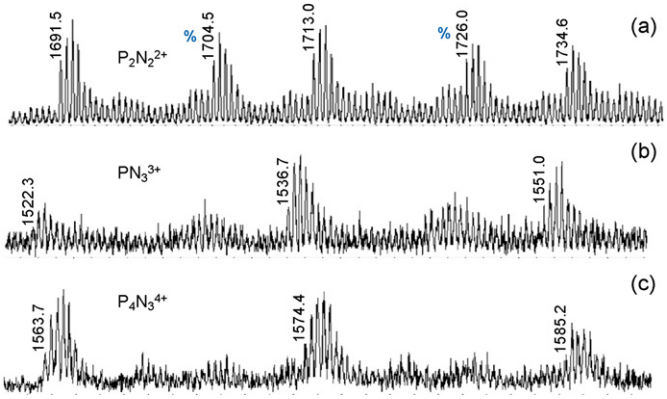

Fig. 8. Mass spectra of regions 9 (a), 10 (b) and 11 (c) in the ESI-TWIM-MS diagram of Fig. 7. The *m*/*z* ratios and isotope distributions agree well with the compositions $P_2N_2^{2+}$, PN_3^{3+} and $P_4N_3^{4+}$, respectively. The distributions labeled by % contain one cyclic and one non-cyclic PEI oligomer; all other distributions contain only non-cyclic PEI oligomers. The abundances of *m*/*z* 1691.5 (a), *m*/*z* 1536.7 (b) and *m*/*z* 1563.7 relative to that of *m*/*z* 846.3 (Fig. 1c) are 2.0%, 0.5% and 0.3%, respectively.

the minor $P_2N_2^{2+}$ distribution (cf. Figs. 1c and 8c), which explains the appearance of several P^+ fragments in the MS^2 spectra of mass-selected PN^+ oligomers (cf. Fig. 6).

4. Conclusions

Our study represents the first microstructure characterization of polyplexes composed of poly(ethylene imine) and oligodeoxynucleotides by ESI mass spectrometry. For the polymer and ODN sizes investigated, the polyplex with 1:1 polymer-to-ODN stoichiometry, PN, is the principal product independent of the reactant mixing ratio. Complexes with the stoichiometries PN_2 and P_2N are formed as minor products, their yields increasing with the concentration of oligonucleotide and polymer, respectively. Other compositions (such as P_2N_2 and PN_3) are formed in trace amounts that are detectable only after charge state deconvolution using TWIM-MS.

The relative intensities of the polyplex ions in ESI mass spectra are shown to reflect the corresponding polyplex solution stabilities; a similar relationship has been reported for the relative intensities of DNA duplexes [13,17,18] and ODN-drug conjugates [16]. The solution and gas-phase stabilities of the polyplexes studied follow identical orders, consistent with very similar structures in both phases. With the polymer systems studied (PEI 400 and 800), thymine-rich nucleotides give rise to the most stable and adenine-rich nucleotides to the least stable polyplexes. This selectivity suggests that polymer structure and size may be tuned to favor complex formation with specific nucleic acid sequences.

Our current study encompassed pentadeoxynucleotides and low molecular weight PEIs. Future studies will probe larger polyplex constituents, other cationic polymers (for example, poly(lysine) or poly(ethylene imine)–poly(ethylene oxide) copolymers), ODNs with different sequences (but rich in specific nucleobases) and single- vs. double stranded ODNs. Dissecting the effect of such determinants on polyplex composition and stability could lead to the design of more efficient transfection vectors.

Acknowledgements

We are grateful to the National Science Foundation for financial support (grants CHE-0517909 and CHE-0833087 for this project and DMR-8821313 for the purchase of the Synapt mass spectrometer). We thank Mr. Vincenzo Scionti and Dr. Nilüfer Solak for experimental assistance and helpful discussions.

References

[1] P.L. Kan, A.G. Schätzlein, I.F. Uchegbu, in: I.F. Uchegbu, A.G. Schätzlein (Eds.), Polymers in Drug Delivery, CRC Press, Boca Raton, 2006, p. 183.
[2] S. Zhang, Y. Xu, B. Wang, W. Qiao, D. Liu, Z. Li, J. Control. Release 100 (2004) 165.
[3] K. Remaut, B. Lucas, K. Raemdonck, K. Braeckmans, J. Demeester, S.C. De Smedt, Biomacromolecules 8 (2007) 1333.
[4] M.T. Nyunt, C.W. Dicus, Y.-Y. Cui, M.C. Yappert, T.R. Huser, M.H. Nantz, J. Wu, Bioconjug. Chem. 20 (2009) 2047.
[5] C.-X. He, Y. Tabata, J.-Q. Gao, Int. J. Pharm. 386 (2010) 232.
[6] K. Itaka, T. Ishii, Y. Hasegawa, K. Kataoka, Biomaterials 21 (2010) 3707.
[7] P. Terrier, J. Tortajada, G. Zin, W. Buchmann, J. Am. Soc. Mass Spectrom. 18 (2007) 1977.
[8] J.B. Fenn, M. Mann, C.K. Meng, S.F. Wong, C.M. Whitehouse, Science 246 (1989) 64.
[9] S.D. Pringle, K. Giles, J.L. Wildgoose, J.P. Williams, S.E. Slade, K. Thalassinos, R.H. Bateman, M.T. Bowers, J.H. Scrivens, Int. J. Mass Spectrom. 261 (2007) 1.
[10] K. Giles, S.D. Pringle, K.R. Worthington, D. Little, J.L. Wildgoose, R.H. Bateman, Rapid Commun. Mass Spectrom. 18 (2004) 2401.
[11] J. Laskin, E. Denisov, J. Futrell, J. Am. Chem. Soc. 122 (2000) 9703.
[12] V. Gabelica, E. De Pauw, J. Mass Spectrom. 36 (2001) 397.
[13] S. Pan, X. Sun, J.K. Lee, J. Am. Soc. Mass Spectrom. 17 (2006) 1383.
[14] L.A. Deschenes, D.A. Vanden Bout, J. Am. Chem. Soc. 122 (2000) 9567.
[15] K.X. Wan, M.L. Gross, T. Shibue, J. Am. Soc. Mass Spectrom. 11 (2000) 450.
[16] K.X. Wan, T. Shibue, M.L. Gross, J. Am. Chem. Soc. 122 (2000) 300.
[17] V. Gabelica, F. Rosu, C. Houssier, E. De Pauw, Rapid Commun. Mass Spectrom. 14 (2000) 464.
[18] X. Sun, J.K. Lee, J. Org. Chem. 75 (2010) 1848.
[19] E. Rivera-Tirado, Association and Fragmentation Characteristics of Biomolecules and Polymers Studied by Mass Spectrometry, Ph.D. Dissertation, The University of Akron, 2007, p. 81.
[20] C.-H. Lee, Y.-H. Ni, C.-C. Chen, C.-K. Chou, F.-H. Chang, Biochim. Biophys. Acta 1611 (2003) 55.
[21] C. Puglisi, F. Samperi, S. Carroccio, G. Montaudo, Rapid Commun. Mass Spectrom. 13 (1999) 2268.
[22] C. Puglisi, F. Samperi, S. Carroccio, G. Montaudo, Polym. Prepr. 41 (1) (2000) 653.
[23] G. von Helden, M.-T. Hsu, P.R. Kemper, M.T. Bowers, J. Chem. Phys. 95 (1991) 3835.
[24] M.T. Bowers, P.R. Kemper, G. von Helden, P.A.M. van Koppen, Science 260 (1993) 1446.
[25] D.E. Clemmer, M.F. Jarrold, J. Mass Spectrom. 32 (1997) 577.
[26] J.A. McLean, B.T. Ruotolo, K.J. Gillig, D.H. Russell, Int. J. Mass Spectrom. 240 (2005) 301.
[27] T. Wyttenbach, M.T. Bowers, Annu. Rev. Phys. Chem. 58 (2007) 511.
[28] A.B. Kanu, P. Dwivedi, M. Tam, L. Matz, H.H. Hill Jr., J. Mass Spectrom. 43 (2008) 1.
[29] L.S. Fenn, J.A. McLean, Anal. Bioanal. Chem. 391 (2008) 905.
[30] B.C. Bohrer, S.I. Merenbloom, S.L. Koeniger, A.E. Hilderbrand, D.E. Clemmer, Annu. Rev. Anal. Chem. 1 (2008) 1.
[31] S. Trimpin, D.E. Clemmer, Anal. Chem. 80 (2008) 9073.
[32] D.E. Clemmer, S.J. Valentine, Nat. Chem. 1 (2009) 257.
[33] Y.-T. Chan, X. Li, M. Soler, J.-L. Wang, C. Wesdemiotis, G.R. Newkome, J. Am. Chem. Soc. 131 (2009) 16395.
[34] J.A. McLean, J. Am. Soc. Mass Spectrom. 20 (2010) 1775.